

Article

Enhancing Flotation Performance of Low-Rank Coal Using Environment-Friendly Vegetable Oil

Mengdi Xu ¹, Ying Zhou ^{1,2}, Yesheng Hao ^{1,2}, Yijun Cao ^{1,3}, Yaowen Xing ^{1,*} and Xiaohui Gui ¹ 

¹ Chinese National Engineering Research Center of Coal Preparation and Purification, China University of Mining and Technology, Xuzhou 221116, China; cumtxmd@outlook.com (M.X.); cumtzhouying@163.com (Y.Z.); haoyesheng1998@163.com (Y.H.); yijuncao@126.com (Y.C.); guixiahui1985@163.com (X.G.)

² School of Chemical Engineering and Technology, China University of Mining and Technology, Xuzhou 221116, China

³ Henan Province Industrial Technology Research Institute of Resources and Materials, Zhengzhou University, Zhengzhou 450001, China

* Correspondence: cumtxyw@cumt.edu.cn; Tel.: +86-15062114600

Abstract: Flotation is widely used for low-rank coal upgrading, although it is always inefficient due to its rough surface morphology and rich oxygen-containing functional groups. In this study, the environment-friendly vegetable oil 1030# was used to enhance the flotation performance of low-rank coal. The mechanism of 1030# enhancing the flotation of low-rank coal was revealed through surface property analysis of coal particles and bubble–particle adhesion tests. The flotation results showed that the flotation yield of low-rank coal increased with the increase in the collector dosage, and the flotation yield of 1030# as a collector is obviously higher than that of diesel. Scanning electron microscopy (SEM) and chromatography–mass spectrometry (GC-MS) were used to analyze the surface morphology of coal particles and components of the reagent. The SEM results showed that the surface of low-rank coal is loose and contains a large number of pores and cracks, which is not conducive to the spreading of chemicals on the coal surface and the mineralization of bubbles and particles. GC-MS results showed that 1030# mainly contained methyl oleate with more unsaturated double bonds than diesel. Fourier transform infrared spectroscopy (FTIR) and X-ray photoelectron spectroscopy (XPS) were used to analyze the surface functional groups of the low-rank coal before and after reagent treatment. The results of FTIR and XPS showed that the coal surface of low-rank coal before reagent treatment contained a large number of oxygen-containing functional groups with poor surface hydrophobicity, while the surface of low-rank coal after reagent treatment had reduced oxygen-containing functional groups and increased hydrophobicity. The contact angle of the low-rank coal surface also showed the same variation trend as the FTIR and XPS results. The adhesion force between the bubble and coal surface in different collector solutions was measured. The maximum adhesion between the bubble and coal surface increased with the increase in the collector, and the maximum adhesion force with 1030# treatment was higher than that of diesel. This indicated that 1030# with a large number of polar components is more easily spread on the surface of low-rank coal, thus improving the hydrophobicity of low-rank coal.

Keywords: low-rank coal; flotation; environment-friendly; vegetable oil; adhesion force



Citation: Xu, M.; Zhou, Y.; Hao, Y.; Cao, Y.; Xing, Y.; Gui, X. Enhancing Flotation Performance of Low-Rank Coal Using Environment-Friendly Vegetable Oil. *Minerals* **2023**, *13*, 717. <https://doi.org/10.3390/min13060717>

Academic Editor: Hyunjung Kim

Received: 23 April 2023

Revised: 16 May 2023

Accepted: 20 May 2023

Published: 24 May 2023



Copyright: © 2023 by the authors. Licensee MDPI, Basel, Switzerland. This article is an open access article distributed under the terms and conditions of the Creative Commons Attribution (CC BY) license (<https://creativecommons.org/licenses/by/4.0/>).

1. Introduction

Coal is the predominant fossil fuel in China, and it is expected to maintain its dominant position in the country's energy structure for the foreseeable future [1–4]. In recent years, rapid industrial development has led to the depletion of high-quality coal resources. Conversely, although the reserves of low-rank coal are abundant, its effective utilization has not been realized to a great extent [2,5]. In economically underdeveloped regions,

the direct combustion of low-rank coal gives rise to the release of various pollutants, including sulfur compounds, nitrogen oxides, and heavy metals, thereby contributing to environmental pollution. Additionally, this combustion process leads to the generation of a significant volume of ash solid waste [6–9]. Therefore, the rational development and clean utilization of this resource is critical to country's economic development and environmental protection. Several separation methods, such as magnetic aspiration, gravity separation, bio-beneficiation and froth flotation, have been developed to facilitate clean and efficient utilization of low-rank coal. Compared with other separation methods, froth flotation is an effective separation method for fine coal cleaning, which depends upon the differences in the surface properties of coal and gangue minerals [10–13].

In the process of fine coal flotation, non-polar hydrocarbon oil is commonly utilized as the collector to enhance the surface hydrophobicity of particles, thereby increasing the probability of bubble–particle adhesion. Low-rank coal, characterized by well-developed pores and an abundance of oxygen-containing functional groups, including hydroxyl, carbonyl and carboxyl moieties [2,10,14], could form stable hydration films on its surface by combining with polar water molecules [15]. This hydration film impedes the spread of the collector on the particle surface, thereby leading to an increased amount of collector dosage and significant rise in economic cost. The low efficiency of flotation, large amount of the collector and high cost are the main problems restricting the efficient utilization of fine low-rank coal.

The high cost of low-rank coal flotation using diesel or kerosene as the collector significantly restricts the improvement in the economic efficiency of the coal plant [16,17]. In recent years, the research on strengthening the flotation process of low-rank coal has attracted extensive attention, especially the development of polar collectors containing oxygen such as alcohols, aldehydes, acids and esters, has aroused great interest from researchers [18]. The addition of a polar collector can modify the surface of low-rank coal, promote the interaction between particles and bubbles and improve the flotation recovery. Jia and Gui et al. [19,20] discovered that the polar groups within the collector could interact with the polar hydrophilic sites present on the coal surface through hydrogen bonding, which can enhance the surface hydrophobicity of the coal sample, consequently leading to an increase in the flotation recovery. Xia et al. [21] found that the lubricating oil, including oxygen-containing functional groups, aromatics and long-chain hydrocarbons, can strongly interact with low-rank coal to improve its surface hydrophobicity. Zhu et al. [22] found that a mixture of fossil oil and oxygen-containing compound (FO) could enhance the low-rank coal flotation compared with traditional diesel oil. The FO was more likely adsorbed on the coal surface, and improved the hydrophobicity of the coal surface, thus promoting the adhesion between bubble and particle. According to previous research, it has been demonstrated that the polar compound collector, a blend of hydrocarbon oil and polar reagent, represents the optimal choice in practical terms. However, it is widely recognized that diesel, kerosene and other fossil oil, which are commonly used as collectors, are non-renewable resources that are expected to become depleted in the near future. Furthermore, these petroleum-derived compounds are not environment-friendly and may entail numerous environmental hazards [23]. In light of these issues, there is a pressing need to explore alternative, renewable and environment-friendly collectors. Vegetable oils, such as colza oil, sunflower oil, soybean oil and olive oil, have been reported as effective collectors for fine coal flotation, owing to their abundant long-chain fatty acids [24–28]. The use of vegetable oils as collectors for low-rank coal flotation presents a significant opportunity for large-scale upgrading of low-rank coal flotation.

In this study, a homemade vegetable oil (1030#) and traditional hydrocarbon oil (diesel) were used as the collectors, and low-rank coal from the coal preparation plant in Zhuanlong Bay was selected as the sample material. The study aims to systematically investigate the underlying mechanisms behind the enhanced flotation of low-rank coal induced by vegetable oil collectors, thereby providing a fundamental basis for the development of new and environment-friendly collectors for low-rank coal flotation.

2. Materials and Methods

2.1. Coal Samples

The coal samples used in the experiment were from low-rank coal, and were collected from Zhuanlong Bay Coal Preparation Plant, Inner Mongolia, China. The proximate analysis result is listed in Table 1. M_{ad} and A_{ad} represent the moisture and ash content, respectively, based on air drying. V_{daf} and F_{daf} are the contents of volatile matter and the fixed carbon on the dry ash-free basis, respectively. The M_{ad} was 11.47%, which indicated the low-rank coal has high water content. The ash content was 17.68%, which was relatively high and required a de-ashing treatment before combustion. The dry ash-free volatile matter content was 35.02%, which indicated that the coal sample belongs to high-volatile coal with a relatively low degree of metamorphism. By referring to the standard of coal classification, the coal sample used in this study should belong to bituminous or sub-bituminous coal as its dry ash-free volatile matter content ranged from 10% to 37% [29]. The wetting screen test was conducted on low-rank coal; the particle size and content distribution of low-rank coal is shown in Figure 1. The 0.50–0.25 mm size is the main size fraction with 31.65% content. Additionally, –0.045 mm size has high yield with 29.14% content, and the ash content of 32.21%. The ash content is correlated with the hydrophilicity of surface, which indicated that flotation recovery of the –0.045 mm fractions is low. The presence of –0.045 mm fractions in the flotation process may not only impede the floatability of coarse coal but also result in clean coal pollution through entrainment and other mechanisms.

Table 1. Proximate analysis of the coal sample.

$M_{ad}/\%$	$A_{ad}/\%$	$V_{daf}/\%$	$FC_{daf}/\%$
11.47	17.68	35.02	64.98

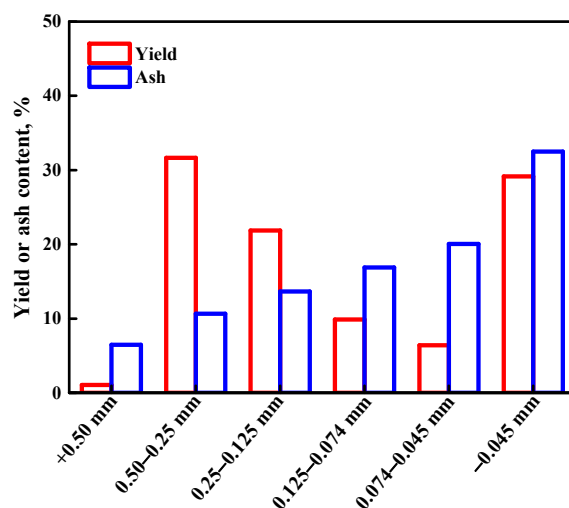


Figure 1. Particle size and ash content distribution of low-rank coal.

Two types of collectors were employed in this experiment: conventional non-polar diesel collector and homemade environment-friendly vegetable oil collector, numbered 1030#. The diesel used in the test was entirely commercial diesel from Sinopec. The 1030# oil utilized was obtained from waste soybean and canola oil sources.

2.2. X-ray Diffractometry Detection (XRD)

X-ray diffractometry (XRD) is a non-destructive technique based on the principle of crystal diffraction, which enables the examination of the internal structure of a sample. By measuring the intensity of diffraction peaks, valuable insights into the crystal structure and composition of different minerals can be obtained. XRD is commonly employed for

the characterization of coal samples in coal separation studies. In this research, the composition of coal samples was examined and analyzed using the D8ADVANCE instrument manufactured by Bruker in Karlsruhe, Germany, operating at a test voltage of 40 kV. The coal particles were required to pass through a 325-mesh screen prior to analysis.

2.3. Scanning Electron Microscope Test

The COXEM-EM30 scanning electron microscopy (SEM, COXEM, Daejeon, Republic of Korea) was conducted to image the surface morphologies of low-rank coal. To enhance surface conductivity, a gold layer was sputter-coated onto the low-rank coal sample prior to SEM imaging. The SEM was operated at a working voltage of 16 kV, a working distance (WD) of 6.9 mm and magnifications of 1000, 2000 and 5000, respectively.

2.4. Gas Chromatography—Mass Spectroscopy Test

Gas chromatography–mass spectrometry (GC-MS) is a potent analytical technique that enables both qualitative and quantitative analysis of individual constituents within a substance. Its exceptional selectivity, and high separation efficiency and sensitivity make it a widely used tool for separating and detecting volatile substances. For the present investigation, a GC-MS system (GCMS-QP2020Nx, Shimadzu, Kyoto, Japan) was employed to characterize the primary constituents of the homemade vegetable oil collector 1030#. The relative mass fractions of the identified components in the collector were determined using the peak area normalization method.

2.5. Flotation Kinetic Experiment

The flotation kinetic experiments were conducted utilizing an XFD-1.0 L laboratory flotation machine (Jilin Exploration Machinery Plant, Changchun, China) to investigate the flotation behavior of low-rank coal. Initially, a mixture of 80 g of low-rank coal and 1 L of deionized water was mixed and pre-wetted for 2 min. The collector reagent, a homemade 1030# reagent and diesel were used as collectors at dosages of 500, 1000, 2000 and 4000 g/t. The frother reagent, octanol, was employed at a dosage of 500 g/t. The collector and frother conditioning periods were 2 and 1 min, respectively. The impeller speed was set at a constant rate of 1800 r/min, while the air flow rate was maintained at 0.1 m³/h. The flotation process was carried out for a duration of 3 min, and the flotation concentrates were collected after 20, 40, 80, 120 and 180 s. Subsequently, the flotation concentrates and tailings were filtered, dried at 80 °C and subjected to further analysis.

2.6. Fourier Transform Infrared Spectroscopy Test

FTIR spectroscopy (Nicolet is5, Thermo Scientific, Waltham, MA, USA) was employed to analyze the chemical functional groups present in coal particles that had been subjected to different chemical treatments, utilizing the wave number range of 4000–400 cm^{−1}. The procedure involved mixing 2 mg of low-rank coal samples with 300 mg of KBr and grinding the resulting mixture to a particle size of 2 µm using an agate mortar. The powdered mixture was then pressed at 30 Mpa pressure to produce thin, circular plates. Lastly, all spectra were subjected to baseline correction.

2.7. X-ray Photoelectron Spectroscopy Test

X-ray photoelectron spectroscopy (XPS) was employed to elucidate the functional groups present on the coal surface in an ultrahigh vacuum (UHV) environment, utilizing a commercially available XPS system (ESCALAB 250Xi, Thermo Scientific, Waltham, MA, USA). The acquired XPS data offered comprehensive insights into the surface physicochemical properties of low-rank coal that had undergone distinct chemical treatments. Subsequent data analysis involving peak fitting was carried out using the XPS Peakfit software, and the binding energies were calibrated relative to the C1s hydrocarbon (C-C/C-H) peak, set at 284.6 eV.

2.8. Contact Angle Measurement

Contact angle measurement is widely used method to evaluate the surface wettability of minerals, and it has been shown that the minerals with larger contact angles exhibit better floatability properties. In this study, we investigated the influence of varying reagent quantities on the wettability of coal samples by utilizing different collectors for the purpose of pulping, filtering and drying the coal samples. To prepare the coal samples for testing, a YP-2 tablet press and boric acid were utilized to create polished coal slices, and the droplet shape analyzer (DSA100, KRUSS, Hamburg, Germany) was employed to perform contact angle measurements. To minimize the experimental error, each testing was repeated five times.

2.9. Bubble—Particle Interaction Measurement

The high-sensitivity microelectromechanical balance system (JK99M2, POWEREACH, Shanghai, China) in conjunction with a digital camera was utilized to investigate the interaction force between bubble and particle under different types and concentrations. The working principle of the JK99M2 can be referred to in paper of Zhu and Li et al. [30,31]. Specifically, low-rank coal flake samples treated with various agents were placed in a transparent tank, and a specific quantity of water was added. The samples were then fixed to the displacement platform situated below the microbalance. A 2 mL bubble was generated at the capillary port of the microbalance, and the force was initialized to 0 at the onset of interaction between bubble and particle. The displacement platform was then gradually moved upwards at a rate of 0.01 mm/s. Upon contact between the coal slice fixed on the displacement platform and bubbles, an instantaneous adhesive force was generated. After the coal samples had moved upwards by 0.3 mm, the sample stage was adjusted to return to its original position at the same speed. To ensure the precision and accuracy of the experimental outcomes, the interaction force measurement was repeated five times to minimize the experimental error.

3. Results and Discussion

3.1. Analysis of Properties for Raw Coal

3.1.1. XRD Result of Raw Coal

In order to ascertain the mineral composition of the low-rank coal sample, X-ray diffractometry (XRD) was employed to conduct phase analysis, and the obtained results are illustrated in Figure 2. The analysis indicated that quartz is the predominant mineral component in the coal sample, accompanied by a minor presence of beryl and polyolithionite, along with other silica-rich minerals. Considering that quartz exhibits strong hydrophilicity and limited adherence to air bubbles during the flotation process, it is more likely to be discarded as tailings.

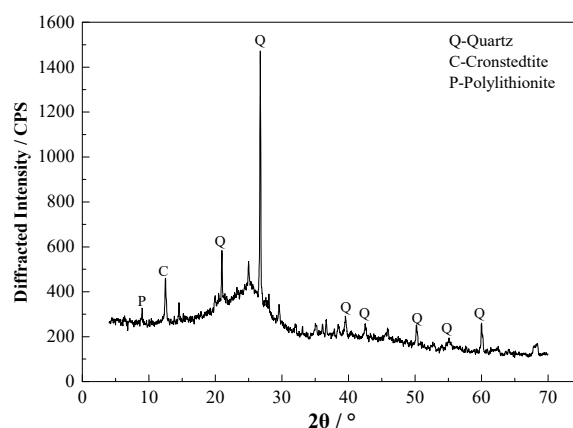


Figure 2. The X-ray diffraction spectrogram of low-rank coal.

3.1.2. Surface Morphology of Raw Coal

The SEM can be used to directly observe the pore, crack and other morphological characteristics on the coal surface. The magnification of SEM was 1000, 2000 and 5000 times, and the surface morphology of low-rank coal is shown in Figure 3. As depicted in Figure 3, the surface of low-rank coal exhibits a rough and porous surface, owing to the presence of numerous pores and cracks, with fine particles adhering to its surface. The formation of low-rank coal involves insufficient pressure and heat exposure to the coal seam, thereby limiting the complete compaction of vegetation debris. Consequently, low-rank coal is characterized by a well-developed porous structure. During the flotation process, capillary pressure attracts flotation agents to penetrate the pores of the coal sample, thereby affecting the spreading of the agents on the sample surface and resulting in excessive consumption [32,33]. The low-rank coal samples used in this paper were relatively uniform without grinding treatment, so the influence of surface roughness changes on flotation can be ignored [34–36].

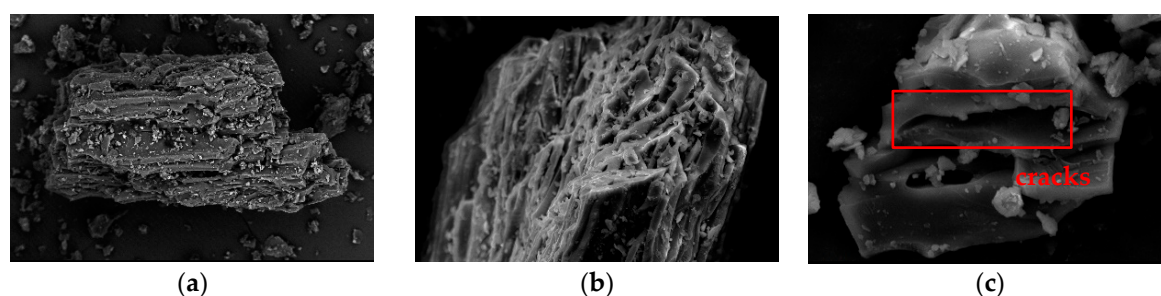


Figure 3. The surface morphology of low-rank coal with different magnifications of SEM, and the magnifications are (a) 1000; (b) 2000; (c) 5000.

3.2. GC-MS Results of Homemade Vegetable Oil 1030#

The chemical constituents of 1030# were subjected to quantitative analysis by GC-MS. The result of the GC/MS analysis of 1030# is presented in Table 2. The chemical profile of 1030# collector is characterized by a highly diverse composition, consisting predominantly of fatty acids and acids, with trans-methyl oleate as the most abundant constituent at 40.22% relative content. In contrast, diesel is primarily composed of alkanes, cycloalkanes and aromatic compounds, as reported by Yang et al. [33]. Fatty acids contain a lot of oxygen-containing groups, and the oxygen-containing groups can form hydrogen bonds with the hydrophilic sites on the surface of low-rank coal, effectively promoting the dispersion of the reagent and the interaction with the coal surface, so as to improve the hydrophobicity of coal particles and increase the flotation recovery, as noted by Xia and Wen et al. [18,37]. Compared to diesel, the use of 1030# collector is expected to result in a more pronounced impact on the floatability of low-rank coal.

Table 2. List of chemical compositions of 1030#.

Retention Time/min	Component	Content/%	Retention Time/min	Component	Content/%
18.608	Trans-methyl oleate;	40.22	23.671	Methyl erucic acid	2.86
20.386	Eicosanoic acid methyl ester	8.83	23.872	Methyl tetradecanoate	2.42
20.533	Eicosanoic acid methyl ester	6.93	24.604	Palmitic acid methyl acetate	1.5
21.078	Methyl docoxate	6.6	25.176	Methyl wax	1.35
22.057	Methyl laurate	5.25	25.348	Methyl twenty-three acid vinegar	1.29

3.3. Flotation Results

The flotation results of low-rank coal subject to diesel and 1030# with different concentrations are shown in Figure 4. The flotation cumulative yield increased as the collector dosage increased. Interestingly, the cumulative yield of 1030# was always higher than that of using diesel. When a 4000 g/t dosage was used, a 37.92% cumulative yield was obtained

with diesel, and an 88.56% cumulative yield was obtained with 1030#, which is higher than that with diesel. It should be noted that there was no significant difference in ash content between diesel and 1030#. The flotation results illustrated that the 1030# had better performance than diesel.

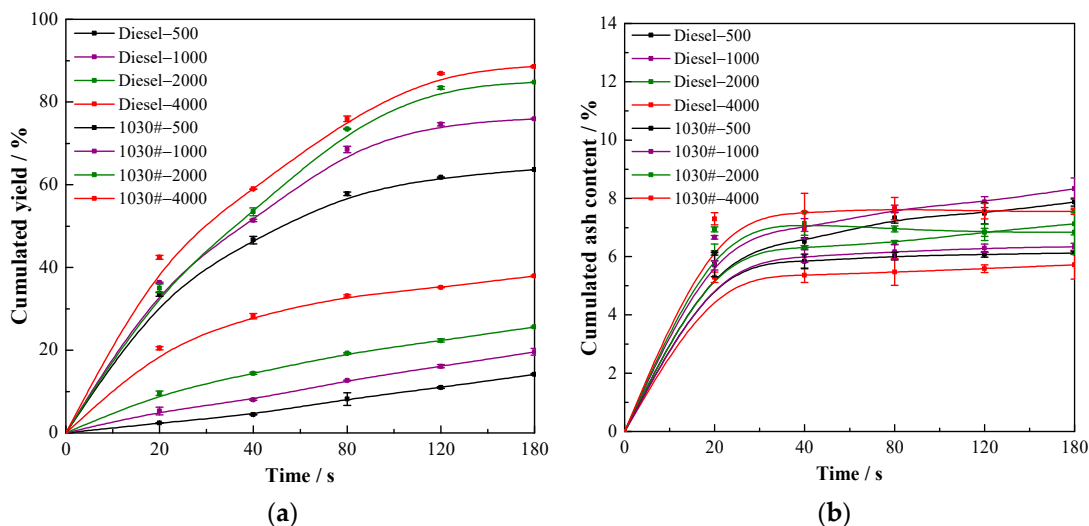


Figure 4. (a) Effect of diesel and 1030# on cumulative yield of low-rank coal flotation. (b) Effect of diesel and 1030# on cumulative ash content of clean coal for low-rank coal flotation.

3.4. Research Results of Enhanced Flotation Mechanism of Vegetable Oil

3.4.1. FTIR Results

The molecular-level information pertaining to the surface functional groups of coal samples treated with various reagents is illustrated in Figure 5, whereas Table 3 exhibits the relative area integration results of the corresponding peaks of the surface functional groups. Figure 5 demonstrates that the infrared spectra of raw coal and coal samples treated with reagents exhibit similar peak positions and shapes, with only differences in peak area and height. It is suggested that there is primarily a physical mechanism of action of these agents on the coal surface, rather than chemical adsorption. The relative integral area results of surface functional groups presented in Table 3 show that reagent treatment resulted in decreased absorption peaks of the ether oxygen bond (C-O) at approximately 1103 cm^{-1} and the carbonyl group (C=O) at around 1702 cm^{-1} . This indicates that the two collectors masked oxygen-containing functional groups on the coal surface, with the 1030# exhibiting a superior performance. The absorption peak near 3695 cm^{-1} and 3602 cm^{-1} also decreased slightly, corresponding to the hydroxyl group (OH) absorption peak, although the change was insignificant. The aliphatic methyl ($-\text{CH}_3$) and methylene ($-\text{CH}_2$) at approximately 2918 cm^{-1} and 2846 cm^{-1} , respectively, did not exhibit a discernible trend [33,38]. These results suggest that the two collectors had comparable shielding effects on these functional groups. Therefore, further testing and analysis of these subtle changes were conducted using XPS.

Table 3. Relative peak area of functional groups on coal surface.

Coal Sample	C-O-C	C=O	$-\text{CH}_3$	$-\text{CH}_2$	$-\text{OH}$
Raw coal	9.90	2.14	0.67	0.70	2.14
Diesel oil treatment	6.96	1.48	0.72	0.66	1.78
1030# oil treatment	5.40	0.74	0.77	0.71	1.37

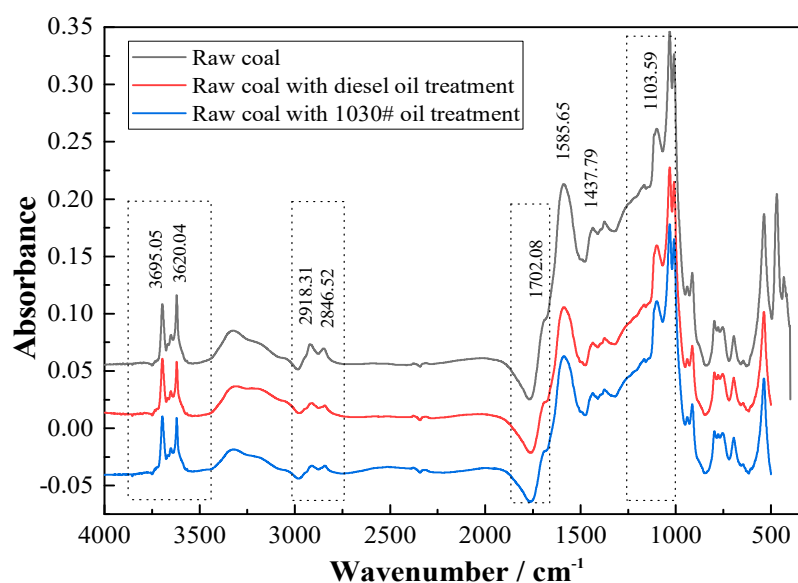


Figure 5. The FTIR results of coal samples with and without reagent treatment.

3.4.2. XPS Results

Figure 6 depicts the X-ray photoelectron spectroscopy (XPS) wide scanning outcomes of both raw coal and coal samples treated with various reagents. Meanwhile, Table 4 demonstrates the corresponding quantification of carbon (C), oxygen (O), aluminum (Al) and silicon (Si) elements. The treatment of low-rank coal with diesel results in an increase in carbon content from 43.92% to 53.79% and a decrease in oxygen content from 39.05% to 33.11%. Similarly, the application of 1030# showed a small increase in the carbon content of 55.67% and a small decrease in the oxygen content of 29.48%. As compared to untreated raw coal, the surface hydrophobicity of low-rank coal is enhanced following reagent treatment, with 1030# exhibiting a superior effect.

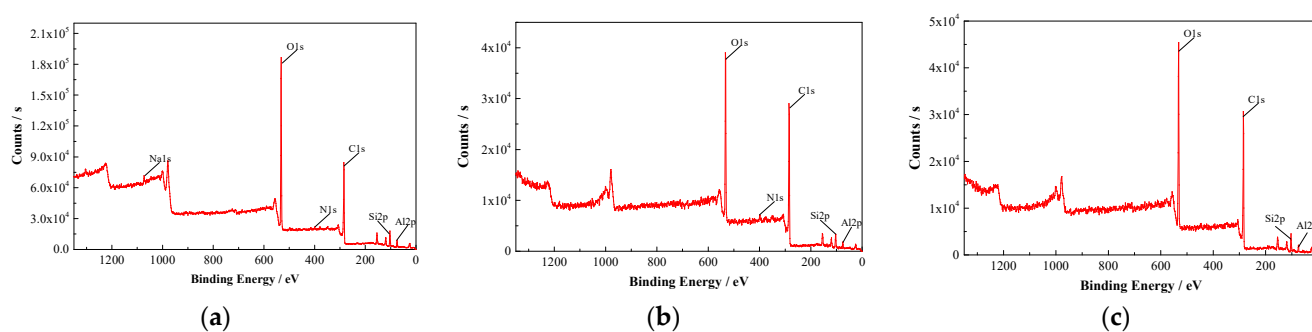


Figure 6. XPS survey scan spectrum of the coal with and without reagent treatment: (a) raw coal, (b) low-rank coal with diesel oil treatment, (c) low-rank coal with 1030# oil treatment.

Table 4. Surface element composition and relative contents of the coal samples with and without reagent treatment.

Relative Contents/%	Types of Elements				
	C	O	Si	Al	Na
Raw coal	43.92	39.05	8.16	6.53	1.29
Diesel oil treatment	53.79	33.11	7.53	5.57	-
1030# oil treatment	55.67	29.48	6.28	4.92	-

The C1s peaks of coal samples are shown in Figure 7. The binding energies of C-C/C-H, C-O, C=O and C=O-O were determined to be 284.60, 285.60, 286.60 and 289.10 eV [3,39], respectively, based on previous studies. The result from the deconvolution of the C peak for coal samples with different reagent treatments is shown in Table 5. With the reagent treatment of low-rank coal, the content of C-C/C-H increased, while the C-O and C=O contents decreased. This trend indicated that the hydrophobicity of low-rank coal was improved after reagent treatment. Compared with diesel, the low-rank coal has higher contents of C-C/C-H and lower contents of C-O, C=O and O=C-O after 1030# treatment. This indicates that the effect of 1030# treatment is more pronounced, which is consistent with the flotation result.

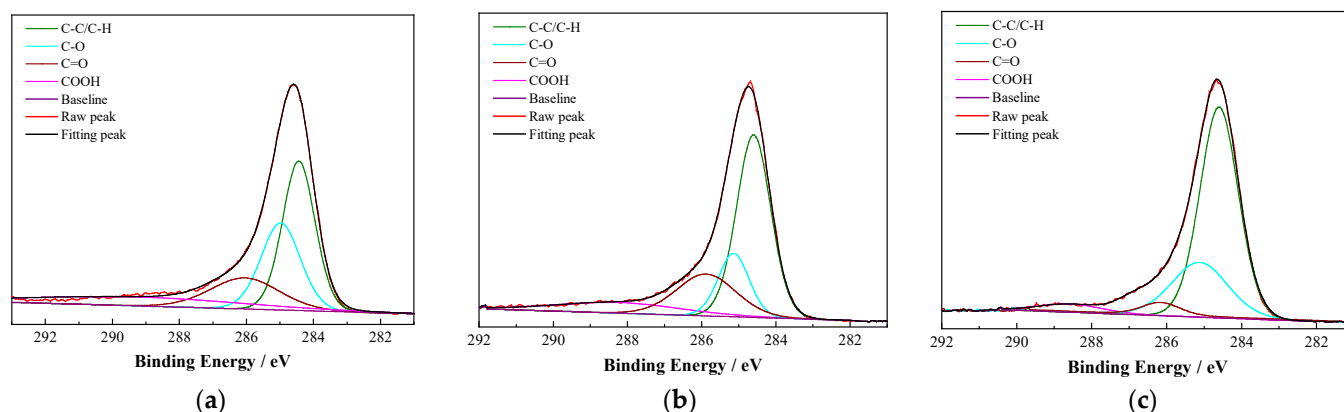


Figure 7. C1s peaks of the coal samples with and without reagent treatment: (a) raw coal, (b) low-rank coal with diesel oil treatment, (c) low-rank coal with 1030# oil treatment.

Table 5. Result of deconvolution of the C peak of coal samples with and without reagent treatment.

Relative Contents/%	Types of Functional Group			
	C-C/C-H	C-O	C=O	C=O-O
Low-rank coal	42.69	32.07	19.34	5.9
Diesel oil treatment	51.99	16.31	20.68	11.01
1030# oil treatment	64.28	28.55	3.65	3.52

3.4.3. Surface Wettability Test Results

The quality of the flotation results is contingent upon the wettability of hydrophobic mineral particles and the surface tension of bubbles in a turbulent fluid flotation environment. The contact angle measurement was employed to investigate the surface wettability of coal samples treated with various reagents. The raw coal sample exhibited a contact angle of 40.25°, whereas the contact angle of coal treated with diesel and 1030# is depicted in Figure 8. Notably, the contact angle increased with a rise in agent dosage, while employing the same collector. Specifically, for a diesel dosage of 500, 1000, 2000 and 4000 g/t, the contact angle increased to 49, 54, 56.9 and 62.5°, respectively. In comparison, for a 1030# dosage of 500, 1000, 2000 and 4000 g/t, the contact angle was 71, 76, 90 and 97°, respectively, which was higher than that of diesel. This result suggests that non-polar hydrocarbon oil does not easily spread on the surface of low-rank coal. Conversely, the polar groups in 1030# tend to be directionally adsorbed to the polar positions of low-rank coal under the influence of hydrogen bonding. It was observed that the higher the hydrophobicity of the coal surface, the greater the contact angle, and consequently, more efficient flotation can be achieved. Additionally, a greater dosage yielded a more prominent effect, which is consistent with the flotation results.

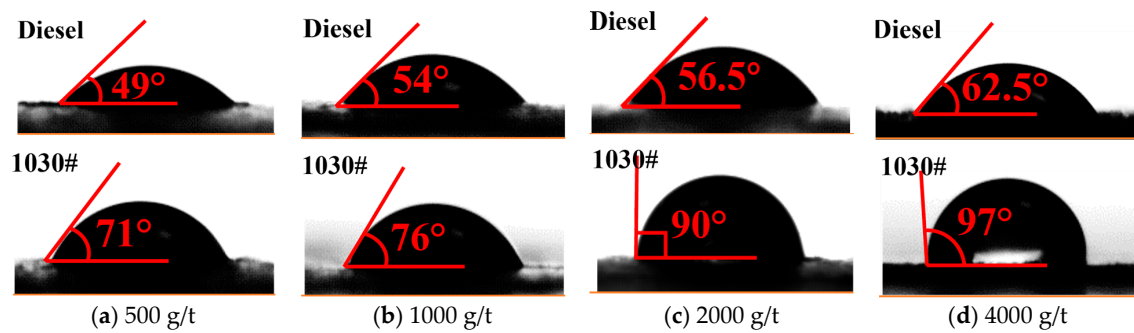


Figure 8. The contact angle of coal samples after diesel and 1030# treatment, and the dosage of diesel and 1030# are: (a) 500 g/t; (b) 1000 g/t; (c) 2000 g/t; (d) 4000 g/t, respectively.

3.4.4. Surface Wettability Test Results

The degree of adhesion between the bubble and coal sample can directly reflect the floatability of coal samples. The interaction between the air bubble and coal surface under different collectors could reveal the performance of the collector on the coal surface [40]. In this study, the force curves of the interaction between bubbles and coal surfaces were investigated at different collector dosages of 500, 1000, 2000 and 4000 g/t, under varying concentrations of diesel and 1030# as shown in Figures 9 and 10. The experimental results demonstrate that the interaction between the bubble and particle underwent several discernible stages. Initially, no force was detected as the bubble approached the coal surface (point A). Subsequently, the bubble made contact with the coal surface (point B) and exerted a downward pressure of 0.3 mm (point C). As the coal sample was subsequently displaced, the bubbles underwent stretching to their maximum extent (point D) before eventually disengaging from the coal surface (point E). Therefore, the force corresponding to point D is the maximum adhesion force between the bubble and coal surface, and the force corresponding to point E is the pull-off force between the bubble and the coal surface.

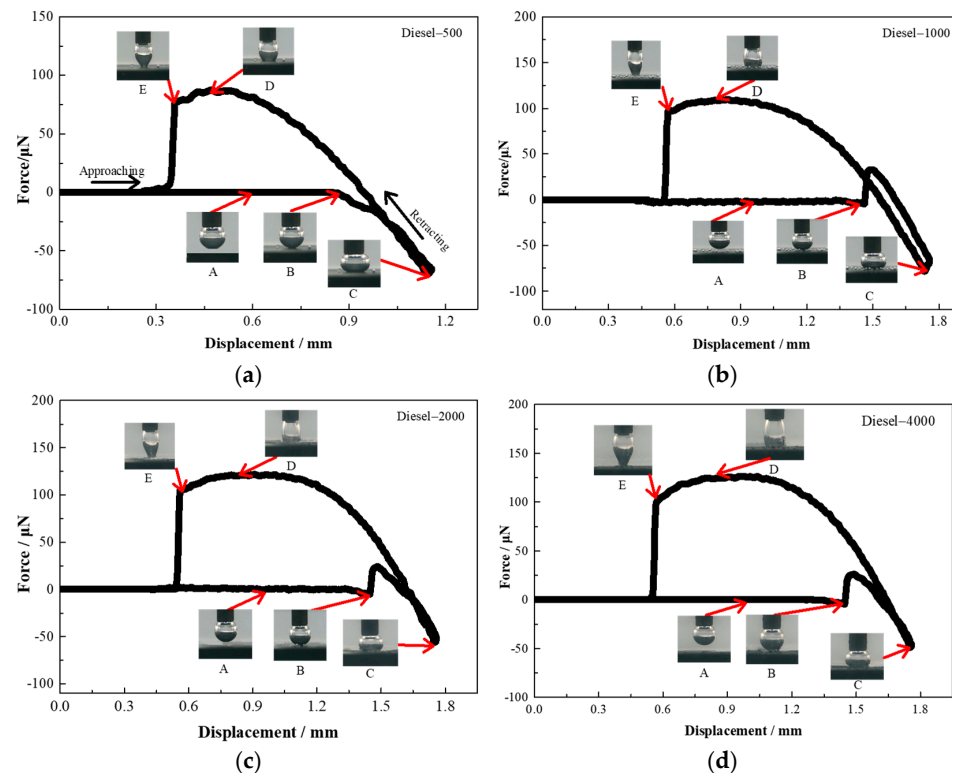


Figure 9. The force curve between bubble and coal surface in different concentrations of diesel solution, (a) 500 g/t; (b) 1000 g/t; (c) 2000 g/t; (d) 4000 g/t.

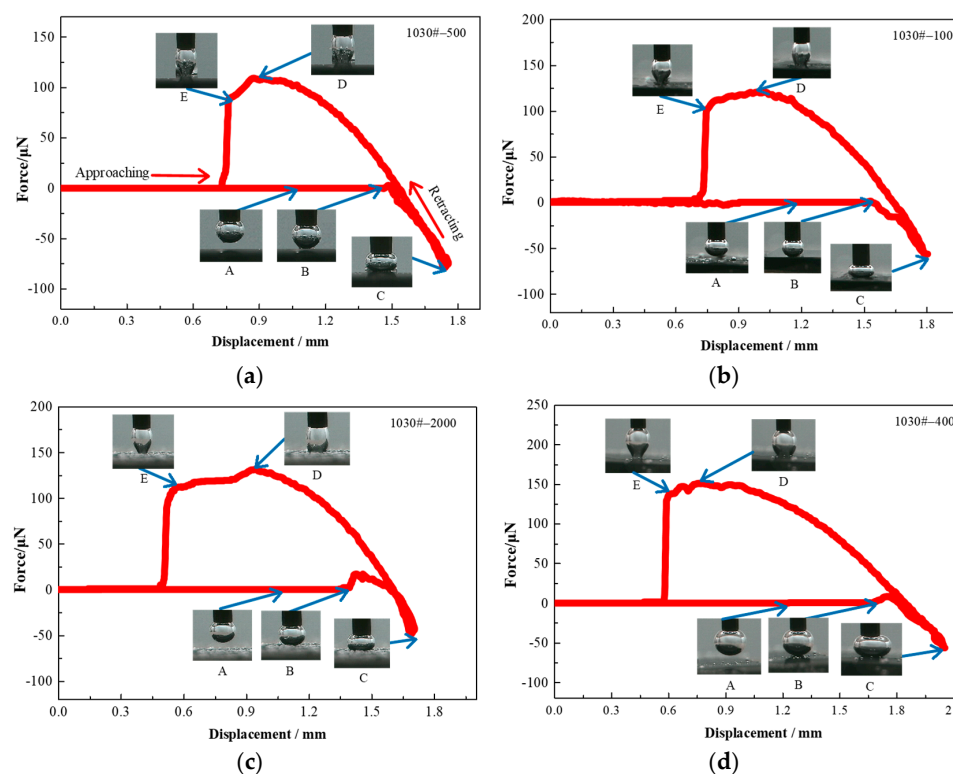


Figure 10. The force curve between bubble and coal surface in different concentrations of 1030# solution, (a) 500 g/t; (b) 1000 g/t; (c) 2000 g/t; (d) 4000 g/t.

The effect of diesel and 1030# concentration on the adhesion force and pull-off force between the bubble and coal samples is presented in Figure 11. The maximum adhesion forces and pull-off forces were determined at diesel dosages of 500, 1000, 2000 and 4000 g/t. The maximum adhesion forces were found to be 87.49, 109.90, 121.69 and 126.64 μN , while the maximum pull-off forces were measured at 76.68, 97.00, 99.82 and 101.54 μN , respectively. Similarly, the maximum adhesion forces and pull-off forces were measured at 1030# dosages of 500, 1000, 2000 and 4000 g/t. The maximum adhesion forces were found to be 109.72, 120.43, 131.40 and 150.87 μN , while the maximum pull-off forces were measured at 88.72, 100.31, 110.14 and 137.63 μN , respectively. Notably, the maximum adhesion force was generally observed to be higher when 1030# was utilized as a collector, as compared to diesel. It is important to note that a higher adhesion force between the bubble and particle leads to the enhanced floatability of coal during the flotation process [41]. The variation in hydrophobicity of low-rank coal can be primarily attributed to the difference in the content of polar components presented in the collector. The raw material used for producing the vegetable collector is the oil-rich seed kernel, which contains unsaturated fatty acids and glycerol. The polar components in the collector possess a polar end and a non-polar end. The polar end can interact with the polar sites present on the surface of low-rank coal through hydrogen bonding, thereby exposing the non-polar end and resulting in an increase in the hydrophobicity on the coal surface. This implies that the 1030# agent has a greater affinity towards the polar regions of low-rank coal, leading to the creation of a more hydrophobic coal surface that is conducive to flotation. Additionally, the maximum pull-off force on the coal surface increased with an increase in the dosage of the collector. This suggested that a higher concentration of the collector leads to an increase in the hydrophobicity of the coal surface, making it harder for bubbles and coal particles to separate during the flotation process. This observation favors flotation, as it results in a higher yield of coal particles. Moreover, the trend observed in the pull-off force is consistent with the flotation results.

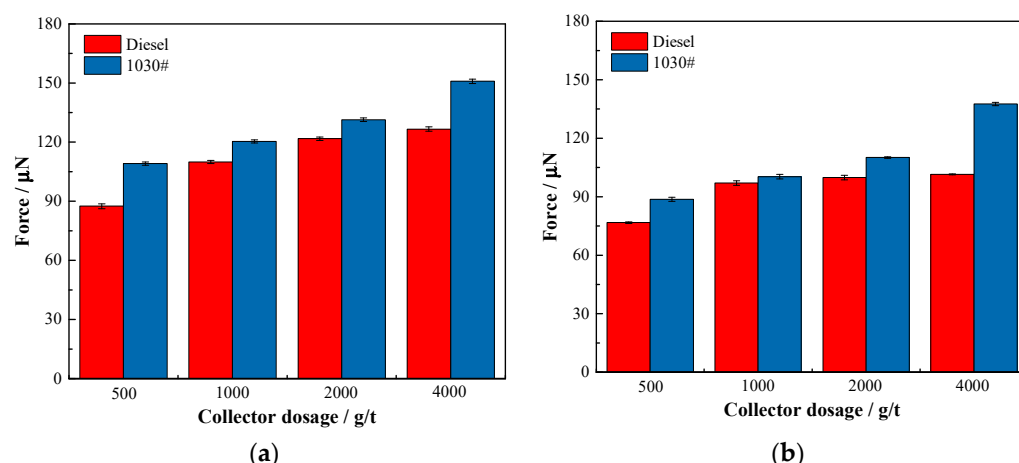


Figure 11. Effect of diesel and 1030# concentration on the adhesion force and pull-off force between bubbles and coal samples, (a) adhesion force between bubbles and coal samples; (b) pull-off force between bubbles and coal samples.

4. Conclusions

Environment-friendly vegetable oil 1030# was used to enhance the flotation performance of low-rank coal in this investigation. The flotation yield using 1030# was always higher than that of using diesel, especially at a high dosage. When a 4000 g/t dosage was used, an 88.56% yield was obtained with 1030#, 50.64% higher than that with diesel. The mechanism of 1030# used as an environment-friendly collector was discussed based on GC-MS, FTIR, XPS and contact angle, and bubble–particle interaction tests. The results of FTIR and XPS analyses revealed a significant decrease in the oxygen content on the surface of coal samples, as well as an increase in the content of hydrophobic functional groups, following treatment with collectors. The results of GC-MS also showed that 1030# contains a large number of polar components; the presence of polar components had a more significant effect due to the adhesion desorption between bubbles and coal particles being enhanced by the presence of polar groups. The contact angle with reagent treatment also increased with the increase in polar components. Additionally, the maximum adhesion force and pull-off force on the coal surface increased with an increase in the content of polar groups. The large number of polar components containing oxygen in vegetable oil easily bonded and interacted with the oxygen-containing functional groups on the surface of low-rank coal under the action of hydrogen bonding, thus increasing the surface hydrophobic area of coal, making it easier to float and improving the flotation efficiency.

Author Contributions: Conceptualization, X.G.; methodology, M.X., Y.Z. and Y.H.; validation, Y.Z. and Y.H.; investigation, M.X. and Y.Z.; resources, Y.C.; data curation, M.X. and Y.Z.; writing—original draft preparation, M.X.; writing—review and editing, M.X. and Y.X.; visualization, M.X. and Y.Z.; supervision, Y.X. and X.G.; funding acquisition, Y.X. and M.X.; All authors have read and agreed to the published version of the manuscript.

Funding: This research was funded by the Jiangsu Natural Science Fund–Youth Fund (Grant no. BK20210500) and the National Nature Science Foundation of China (Grant no. 52104277).

Conflicts of Interest: The authors declare no conflict of interest.

References

1. Lin, B.; Yao, X.; Liu, X. China's energy structure adjustment of under the constraint of energy saving and carbon emission strategy. *Soc. Sci. China* **2010**, *31*, 91–110.
2. Yu, J.; Tahmasebi, A.; Han, Y.; Yin, F.; Li, X. A review on water in low rank coals: The existence, interaction with coal structure and effects on coal utilization. *Fuel Process. Technol.* **2013**, *106*, 9–20. [[CrossRef](#)]
3. Xu, M.; Guo, F.; Zhang, Y.; Yang, Z.; Cao, Y.; Gui, X.; Xing, Y. Effect of hydrothermal pretreatment on surface physicochemical properties of lignite and its flotation response. *Powder Technol.* **2021**, *386*, 81–89. [[CrossRef](#)]

4. Sivrikaya, O. Cleaning study of a low-rank lignite with DMS, Reichert spiral and flotation. *Fuel* **2014**, *119*, 252–258. [\[CrossRef\]](#)
5. Tu, Q.; Cheng, Y.; Xue, S.; Ren, T.; Cheng, X. Energy-limiting factor for coal and gas outburst occurrence in intact coal seam. *Int. J. Min. Sci. Technol.* **2021**, *31*, 729–742. [\[CrossRef\]](#)
6. Pan, J.; Hassas, B.; Rezaee, M.; Zhou, C.; Pisupati, S. Recovery of rare earth elements from coal fly ash through sequential chemical roasting, water leaching, and acid leaching processes. *J. Clean. Prod.* **2021**, *284*, 124725. [\[CrossRef\]](#)
7. Hu, P.; Liang, L.; Xie, G.; Zhou, S.; Peng, Y. Effect of slurry conditioning on flocculant-aided filtration of coal tailings studied by low-field nuclear magnetic resonance and X-ray micro-tomography. *Int. J. Min. Sci. Technol.* **2020**, *30*, 859–864. [\[CrossRef\]](#)
8. Behera, S.; Meena, H.; Chakraborty, S.; Meikap, B. Application of response surface methodology (RSM) for optimization of leaching parameters for ash reduction from low-grade coal. *Int. J. Min. Sci. Technol.* **2018**, *28*, 621–629. [\[CrossRef\]](#)
9. Stańczyk, K.; Bajerski, A.; Czny, M. Negative-pressure pneumatic separator: a new solution for hard-coal beneficiation. *Int. J. Min. Sci. Technol.* **2021**, *8*, 103–123.
10. Xia, W.; Xie, G.; Peng, Y. Recent advances in beneficiation for low rank coals. *Powder Technol.* **2015**, *277*, 206–221. [\[CrossRef\]](#)
11. Ozkan, S. Effects of simultaneous ultrasonic treatment on flotation of hard coal slimes. *Fuel* **2012**, *93*, 576–580. [\[CrossRef\]](#)
12. Liu, J.; Bao, X.; Hao, Y.; Liu, J.; Cheng, Y.; Zhang, R.; Xing, Y.; Gui, X.; Li, J.; Avid, B. Research on mechanisms of improving flotation selectivity of coal slime by adding sodium polyphosphate. *Minerals* **2022**, *12*, 1392.
13. Rong, G.; Xia, Y.; Zhang, Y.; Guo, F.; Wang, D.; Zhang, R.; Xing, Y.; Gui, X. Effect of Comminution methods on low-rank coal bubble-particle attachment/detachment: Implications for flotation. *Minerals* **2019**, *9*, 452. [\[CrossRef\]](#)
14. Tahmasebi, A.; Yu, J.; Han, Y.; Zhao, H.; Bhattacharya, S. A kinetic study of microwave and fluidized-bed drying of a Chinese lignite. *Chem. Eng. Res. Des.* **2014**, *92*, 54–65. [\[CrossRef\]](#)
15. Xia, Y.; Zhang, R.; Xing, Y.; Gui, X. Improving the adsorption of oily collector on the surface of low-rank coal during flotation using a cationic surfactant: An experimental and molecular dynamics simulation study. *Fuel* **2019**, *235*, 687–695. [\[CrossRef\]](#)
16. Jia, R.; Harris, G.; Fuerstenau, D. An improved class of universal collectors for the flotation of oxidized and/or low-rank coal. *Int. J. Min. Sci. Technol.* **2000**, *58*, 99–118. [\[CrossRef\]](#)
17. Atesok, G.; Celik, M. A new flotation scheme for a difficult-to-float coal using pitch additive in dry grinding. *Fuel* **2000**, *79*, 1509–1513. [\[CrossRef\]](#)
18. Wen, B.; Xia, W.; Sokolovic, J. Recent advances in effective collectors for enhancing the flotation of low rank/oxidized coals. *Powder Technol.* **2017**, *319*, 1–11. [\[CrossRef\]](#)
19. Jia, R.; Harris, G.; Fuerstenau, D. Chemical reagents for enhanced coal flotation. *Int. J. Coal Prep. Util.* **2002**, *22*, 123–149. [\[CrossRef\]](#)
20. Gui, X.; Xing, Y.; Wang, T.; Cao, Y.; Miao, Z.; Xu, M. Intensification mechanism of oxidized coal flotation by using oxygen-containing collector α -furanacrylic acid. *Powder Technol.* **2017**, *305*, 109–116. [\[CrossRef\]](#)
21. Xia, Y.; Yang, Z.; Zhang, R.; Xing, Y.; Gui, X. Performance of used lubricating oil as flotation collector for the recovery of clean low-rank coal. *Fuel* **2018**, *239*, 717–725. [\[CrossRef\]](#)
22. Zhu, C.; Xing, Y.; Xia, Y.; Wang, Y.; Li, G.; Gui, X. Flotation intensification of low-rank coal using a new compound collector. *Powder Technol.* **2020**, *370*, 197–205. [\[CrossRef\]](#)
23. Xia, W.; Yang, J.; Liang, C. Improving oxidized coal flotation using biodiesel as a collector. *Int. J. Coal Prep. Util.* **2013**, *33*, 181–187. [\[CrossRef\]](#)
24. Hacifazlioglu, H.; Senol-Arslan, D. Sunflower oil as green collector in bituminous coal flotation. *Energy Sources Part A* **2017**, *39*, 1602–1609. [\[CrossRef\]](#)
25. Alonso, M.; Castano, C.; Garcia, A. Performance of vegetable oils as flotation collectors for the recovery of coal from coal fines wastes. *Int. J. Coal Prep. Util.* **2000**, *21*, 411–420. [\[CrossRef\]](#)
26. Alonso, M.; Valdés, A.; MartíNez-Tarazona, R.; Garcia, A. Coal recovery from coal fines cleaning wastes by agglomeration with vegetable oils: Effects of oil type and concentration. *Fuel* **1999**, *78*, 753–759. [\[CrossRef\]](#)
27. Das, B.; Reddy, P. The utilization of non-coking coal by flotation using non-conventional reagents. *Energy Sources Part A* **2010**, *32*, 1784–1793. [\[CrossRef\]](#)
28. Xu, M.; Xing, Y.; Cao, Y.; Gui, X. Waste colza oil used as renewable collector for low rank coal flotation. *Powder Technol.* **2019**, *344*, 611–616. [\[CrossRef\]](#)
29. Chen, P. Coal classification in China: A complete system (part 1). *China Coal* **2000**, *26*, 5–8.
30. Zhu, C.; Li, G.; Xing, Y.; Gui, X. Adhesion forces for water/oil droplet and bubble on coking coal surfaces with different roughness. *Int. J. Min. Sci. Technol.* **2021**, *31*, 681–687. [\[CrossRef\]](#)
31. Li, M.; Xing, Y.; Zhu, C.; Liu, Q.; Yang, Z.; Zhang, R.; Zhang, Y.; Xia, Y.; Gui, X. Effect of roughness on wettability and floatability: Based on wetting film drainage between bubbles and solid surfaces. *Int. J. Min. Sci. Technol.* **2022**, *32*, 1389–1396. [\[CrossRef\]](#)
32. Xing, Y.; Gui, X.; Cao, Y.; Wang, D.; Zhang, H. Clean low-rank-coal purification technique combining cyclonic-static microbubble flotation column with collector emulsification. *J. Clean. Prod.* **2016**, *153*, 657–672. [\[CrossRef\]](#)
33. Yang, Z.; Chang, G.; Xia, Y.; He, Q.; Zeng, H.; Xing, Y.; Gui, X. Utilization of waste cooking oil for highly efficient recovery of unburned carbon from coal fly ash. *J. Clean. Prod.* **2020**, *282*, 124547. [\[CrossRef\]](#)
34. Guven, O.; Kaymakoglu, B.; Ehsani, A.; Hassanzadeh, A.; Sivrikaya, O. Effects of grinding time on morphology and collectorless flotation of coal particles. *Powder Technol.* **2021**, *339*, 117010. [\[CrossRef\]](#)
35. Yin, W.; Zhu, Z.; Yang, B.; Fu, Y.; Yao, J. Contribution of particle shape and surface roughness on the flotation behavior of low-ash coking coal. *Energy Sources Part A* **2019**, *41*, 636–644. [\[CrossRef\]](#)

36. Gomez-Flores, A.; Bradford, S.; Hwang, G.; Heyes, G.; Kim, H. Particle–bubble interaction energies for particles with physical and chemical heterogeneities. *Miner. Eng.* **2020**, *155*, 106472. [[CrossRef](#)]
37. Xia, Y.; Rong, G.; Xing, Y.; Gui, X. Synergistic adsorption of polar and nonpolar reagents on oxygen-containing graphite surfaces: Implications for low-rank coal flotation. *J. Colloid Interf. Sci.* **2019**, *557*, 276–281. [[CrossRef](#)]
38. Chen, S.; Wang, S.; Li, L.; Qu, J.; Tao, X.; He, H. Exploration on the mechanism of enhancing low-rank coal flotation with cationic surfactant in the presence of oily collector. *Fuel* **2018**, *227*, 190–198. [[CrossRef](#)]
39. Yang, Z.; Guo, F.; Xia, Y.; Xing, Y.; Gui, X. Improved floatability of low-rank coal through surface modification by hydrothermal pretreatment. *J. Clean. Prod.* **2020**, *246*, 119025. [[CrossRef](#)]
40. Yang, H.; Xing, Y.; Sun, L.; Cao, Y.; Gui, X. Kinetics of bubble-particle attachment and detachment at a single-bubble scale. *Powder Technol.* **2020**, *370*, 251–258. [[CrossRef](#)]
41. Sherman, H.; Nguyen, A.; Bruckard, W. An analysis of bubble deformation by a sphere relevant to the measurements of bubble-particle contact interaction and detachment forces. *Langmuir* **2016**, *32*, 12022–12030. [[CrossRef](#)] [[PubMed](#)]

Disclaimer/Publisher’s Note: The statements, opinions and data contained in all publications are solely those of the individual author(s) and contributor(s) and not of MDPI and/or the editor(s). MDPI and/or the editor(s) disclaim responsibility for any injury to people or property resulting from any ideas, methods, instructions or products referred to in the content.